C H A P T E R VII

HARDNESS ANISOTROPY AND ERSS OF RHOMBOHEDRAL CRYSTALS : SODIUM NITRATE AND CALCITE

CHAPTER VII

HARDNESS ANISOTROPY AND ERSS OF RHOMBOHEDRAL CRYSTALS : SODIUM NITRATE AND CALCITE

7.1 INTRODUCTION:

It is well known that the measured hardness of single crystal materials can vary with the orientation of the indenter relative to the material's crystallographic axes, particularly when the indenter is of low symmetry (as is the Knoop indenter). The form of the hardness anisotropy is characteristic of the material's active slip systems, the face indented and the shape of the indenter and various models exist for its prediction /1-4/. Such models have been used to determine the active slip systems in crystals, and can be particularly useful for hard, brittle solids where microhardness testing is virtually the only means of inducing controllable plastic flow at low temperatures /5-7/.

Models of the types used in Refs.1-5 relate the measured hardness at a particular orientation to the inverse of the resolved shear stress applied by each of the indenter facets to the active slip systems, with additional terms to allow for the constraints on flow directions imposed by the presence of the indenter. Any possible variation of workhardening rates with orientation are neglected. These "Effective Resolved Shear Stress" (ERSS) models assume a stress state equivalent to tension along the line of greatest slope in an indenter facet, compression normal to this direction, or some other simplified stress field. ERSS models predict the same variation of hardness with orientation for all materials with the same slip systems, regardless of bonding type, temperature, etc. /8/.

An analytical treatment of this behaviour in terms of localised plastic deformation occurring during indentation has been given by Daniels and Dunn (DD). More recently, the theory has been critically assessed and modified by Brookes, O'Neil and Redfern (BOR). The explanation given by all these authors is based on the premises that the hardness anisotropy is related to the orientation dependence of the effective resolved shear stresses (ERSS) which are acting, during deformation, in those directions that accommodate dislocation movement. According to DD, the ERSS associated with a particular slip system is related to the tensile component F of the applied force acting along each facet of the indenter and is given by:

$$\text{ERSS} = (F/A) \cos \lambda \cos \phi \cos \psi \quad \ldots \quad (7.1)$$

'A' is the area of specimen undergoing deformation,

λ = Angle between tensile stress axis and slip direction.

ϕ = Angle between tensile stress axis and slip plane normal.

ψ = Angle between an axis parallel to the indenter face and the axis of rotation of the slip system during deformation.

The cos ψ term arises as a consequence of material constraints associated with the dimensional changes accompanying deformation (Fig.7.1). The BOR equation is similar to that given by DD, but includes an additional constraint term, sin γ, where γ is the angle between the axis H and the slip direction.

$$\text{ERSS} = (F/A) \cos \lambda \cos \phi \frac{(\cos \psi + \sin \gamma)}{2} \quad \ldots . \quad (7.2)$$

The assessment made by Brookes et al. of Knoop hardness data available in the literature upto 197C confirmed the validity of the theoretical treatment for relatively simple crystals with cubic and hexagonal lattices. In addition it was strongly suggested that crystal with a similar structure had the same slip systems operating during the deformation. Very little has been published on Knoop indentation studies of non-cubic materials having a more complex structure, where other deformation mechanisms (such as twinning) may be dominant. In this context it should be noted that twinning in magnesium has been successfully treated by the Daniels and Dunn method /9/. The present work reports the hardness anisotropy of calcium carbonate (calcite) and sodium nitrate. Both these solids have complex but structurally similar anions and are isomorphous with a rhombohedral structure in which the lattice parameters are almost identical /10/.

It is usual to identify the lattices of both sodium nitrate and calcite by identical tetramolecular unit cells defined by equivalent cleavage faces, designated $\{100\}$. Primary slip systems in calcite have been reported as $\{100\}$ [011] and $\{11\bar{1}\}$ [011] /11,12/ and in addition $\{100\}$ [011] twin gliding is an important deformation process /13/. These systems are also expected to be operative in sodium nitrate /14/.

The variation of hardness with orientation and with quenching temperature was studied in the earlier chapter. The empirical formulae for these variations wer also derived. The present study attempts to determine the variation of ERSS with hardness, i.e., with orientation and quenching temperature and to determine to what extent ERSS models fit with the present data.

7.2 OBSERVATIONS:

The hardness values obtained at different orientations and different quenching temperatures for $NaNO_3$ and $CaCO_3$ cleavages were obtained from the earlier chapter. The angles λ , ϕ , ψ and γ were determined (Table 7.1) by using the standard method of stereographic projection described in the earlier chapter. The stereographic projections used for the determinations of λ , ϕ , ψ and γ are given in Fig.7.1(b). Calculations of the product of cosine and sine terms of (7.2) were made for different orientations. Since ERSS is proportional to this product, it is desirable to follow the graphical method for analysis. The plots of ERSS Vs. orientations (vide table 7.2) for $NaNO_3$ and $CaCO_3$ are shown in Fig.7.2.

7.3 RESULTS AND DISCUSSION:

It is clear from the plot of Knoop hardness number (H) Vs. orientation (A) Fig.7.2(b) that hardness maxima occur at 78° and 156° (a_1 & a_2) and minima at 39°, 117° (b_1 & b_2). In the present case, the directions $[0\bar{1}0]$ and [100] (Fig.7.2(a)) are inclined with each other at an angle of 78°. Thus the hardness maxima are in the directions $\langle 100 \rangle$ (a_1, a_2) and minima along $[1\bar{1}0]$ (b_1, b_2). The primary slip system $\{100\}[011]$ is the one in which the author was interested because ERSS data was calculated for this system only. ERSS Vs. A plot indicates that when ERSS attains a maximum value (d_1, d_2, d_3) the corresponding hardness values for $NaNO_3$ and $CaCO_3$ are having minimum (b_1, b_2, b_3) values corresponding to 17.5 and 100 $kg\text{-}mm^{-2}$ respectively, thus supporting the BOR model. It should be noted that ERSS values were also calculated by using DD equation (7.1). However, the experimental correlation with the calculated values was poor. Hence these plots are not shown in Fig.7.2(b). The hardness anisotropy factors expressed by the ratio of maximum hardness to minimum hardness of cleavage faces of $NaNO_3$ and $CaCO_3$ are 1.4 and 1.2 respectively.

It is interesting to compare the measurements made by the author with those available in the literature. Gallagher et al. /14/ (1987) had made a comparative study of anisotropy in Knoop hardness of $CaCO_3$ and $NaNO_3$ single crystals. Using DD and BOR expressions, the cosine terms or cosine and sine terms were calculated for those systems of slip and twinning detectable on cleavage planes and assumed to be active at each of the four facets of the indenter. An average value was taken. This corresponds to a value of A for $NaNO_3$ and $CaCO_3$. Since the present author had calculated ERSS for one system only, namely, $\{100\}[011]$, comparison will be made for this one only. Since they made graphical presentation on the basis of the symmetry about A = 129°, corresponding to the short diagonal of the rhombic face of a crystal, the present observations were transformed by taking into account their basis (Fig.7.2a). The plots of H Vs. A and ERSS Vs. A were shown in the same diagram (Fig.7.2b). The curves numbered 1, 2, 3 drawn on several experimental points are based on data for H of $NaNO_3$ and $CaCO_3$ and for ERSS of $NaNO_3$ and $CaCO_3$ obtained by the author. The curves 4 and 5 corresponding to data on H of $CaCO_3$ and on ERSS of $CaCO_3$ are taken from the above referred paper by Gallagher et al./14/. They had assumed that the curve based on ERSS of $NaNO_3$ is of the same form as that of calcite for cleavage planes. However, the experimental curve 6 on H of $NaNO_3$ given by them indicates that for a constant applied load of 25 gm, hardness increases with orientation, attains a maximum value (i_1, i_2) at 78° and 180° (or 0°) and a minimum value 129° (h_1) and the reference directions they have chosen are shown in Fig.7.2a. This curve indicates very clearly that for $CaCO_3$, ERSS (curve 5) which has a minimum (f_1, f_2) value corresponding to maximum (g_1, g_2) hardness for this orientation and that for $NaNO_3$, the minimum of ERSS (h_1) corresponds to minimum hardness (j_1) of $NaNO_3$. This observation is diametrically opposite to the one obtained by the author. It is very difficult to explain this anomaly of observations of Gallagher et al. It should be remarked that, no significant mistakes had crept in the calculations reported by the author. Further, the detailed report on variation of hardness with applied load at constant temperature shows very clearly that in HLR, the hardness is independent of load at all loads after 20 gm load. The author has verified that for all other applied loads beyond 20 gm, hardness has a minimum value represented by point j_1 (Fig.7.2b). Hence this shows that experimentally hardness has a minimum value at j_1. It is therefore hard to explain the correspondence of minimum ERSS with minimum hardness of $NaNO_3$ cleavages reported by Gallagher et al.

7.4 CONCLUSIONS:

The ERSS study for primary slips [011] on $NaNO_3$ and $CaCO_3$ cleavage faces $\{100\}$ is correlated with hardness anisotropy of these crystals. For $NaNO_3$ and $CaCO_3$ the hardness maxima correspond to ERSS minima and conversely. The anisotropy factor represented by ratio of maximum hardness to minimum hardness of $NaNO_3$ and $CaCO_3$ in the high load region, i.e., for all applied loads beyond 20 gm load for $NaNO_3$ and 40 gm load for calcite cleavages, is different for these isostructural, isomorphous crystals.

TABLE 7.1 (A)

Orientation	Facet (1) & (3)				Facet (1) & (3)				Facet (1) & (3)			
	(i) (100)[011]				(ii) (010)[011]				(iii) (001)[011]			
A	ϕ°	λ°	ψ°	$\surd^{\circ}$	ϕ°	λ°	ψ°	$\surd^{\circ}$	ϕ°	λ°	ψ°	$\surd^{\circ}$
0	87	65	100	140	18	65	50	140	18	85	50	140
10	87	74	110	136	14	74	51	136	14	74	51	136
20	87	81	120	132	16	81	53	132	16	81	53	132
30	87	89	130	126	22	89	57	126	22	89	57	126
40	87	96	140	120	30	96	62	120	30	96	62	120
50	87	105	150	112	39	105	68	112	39	105	68	112
60	87	112	160	104	48	112	73	104	48	112	73	104
70	87	118	170	96	58	118	80	96	58	118	80	96
80	87	125	180	89	68	125	86	89	68	125	86	89
90	87	130	170	82	77	130	92	82	77	130	92	82
100	87	134	160	74	86	134	99	74	86	134	99	74
110	87	136	150	67	96	136	105	67	96	136	105	67
120	87	136	140	60	107	136	111	60	107	136	111	60
130	87	135	130	54	116	135	117	54	116	135	117	54
140	87	131	120	48	126	131	122	48	126	131	122	48
150	87	126	110	44	135	126	127	44	135	126	122	44
160	87	121	100	41	144	121	130	41	144	121	130	41
170	87	114	90	40	151	114	131	40	151	114	131	40
180	87	106	131	42	157	106	131	42	157	106	131	42

TABLE 7.1 (B)

Orientation	Facet (2) & (4) (i) (100)[011]				Facet (2) & (4) (ii) (010)[011]				Facet (2) & (4) (iii) (001)[011]			
A	ϕ°	λ°	ψ°	γ°	ϕ°	λ°	ψ°	γ°	ϕ°	λ°	ψ°	γ°
0	86	130	113	136	77	130	52	136	46	130	46	136
10	86	134	123	131	86	134	56	131	55	134	44	131
20	86	137	133	125	96	137	60	125	64	137	45	125
30	86	137	143	118	105	137	64	118	74	137	48	118
40	86	136	153	111	115	136	70	111	84	136	51	111
50	86	133	163	104	125	133	76	104	94	133	56	104
60	86	128	173	96	135	128	82	96	104	128	61	96
70	86	122	177	88	143	122	86	88	114	122	66	88
80	86	115	167	80	148	115	95	80	122	115	74	80
90	86	109	158	74	154	109	100	74	132	109	81	74
100	86	102	147	65	159	102	108	65	140	102	89	65
110	86	94	137	58	158	94	114	58	148	94	96	58
120	86	88	127	52	154	88	119	52	154	88	103	52
130	86	79	117	46	145	79	123	46	158	79	110	46
140	86	71	107	42	137	71	127	42	158	71	116	42
150	86	64	97	40	128	64	129	40	153	64	122	40
160	86	56	87	40	119	56	130	40	147	56	128	40
170	86	50	76	42	110	50	130	42	139	50	132	42
180	86	45	66	45	101	45	128	45	131	45	135	45

TABLE 7.2

Orientation A	Average/ERSS (BOR)
0	0.1114
10	0.0886
20	0.0625
30	0.0509
40	0.0836
50	0.1145
60	0.1145
70	0.0836
80	0.0509
90	0.0625
100	0.0886
110	0.1114
120	0.1122
130	0.0893
140	0.06247
150	0.0509
160	0.0836
170	0.11455
180	0.1145

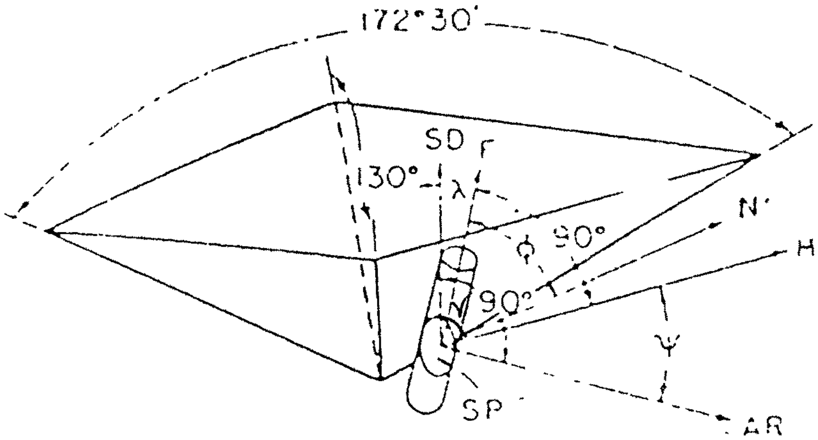

Schematic diagram of the Knoop indenter and cylinder of deformation showing positions of force (F), slip direction (SD), slip plane (SP) and axes of rotation (AR and H)

Fig. 7.1 (a)

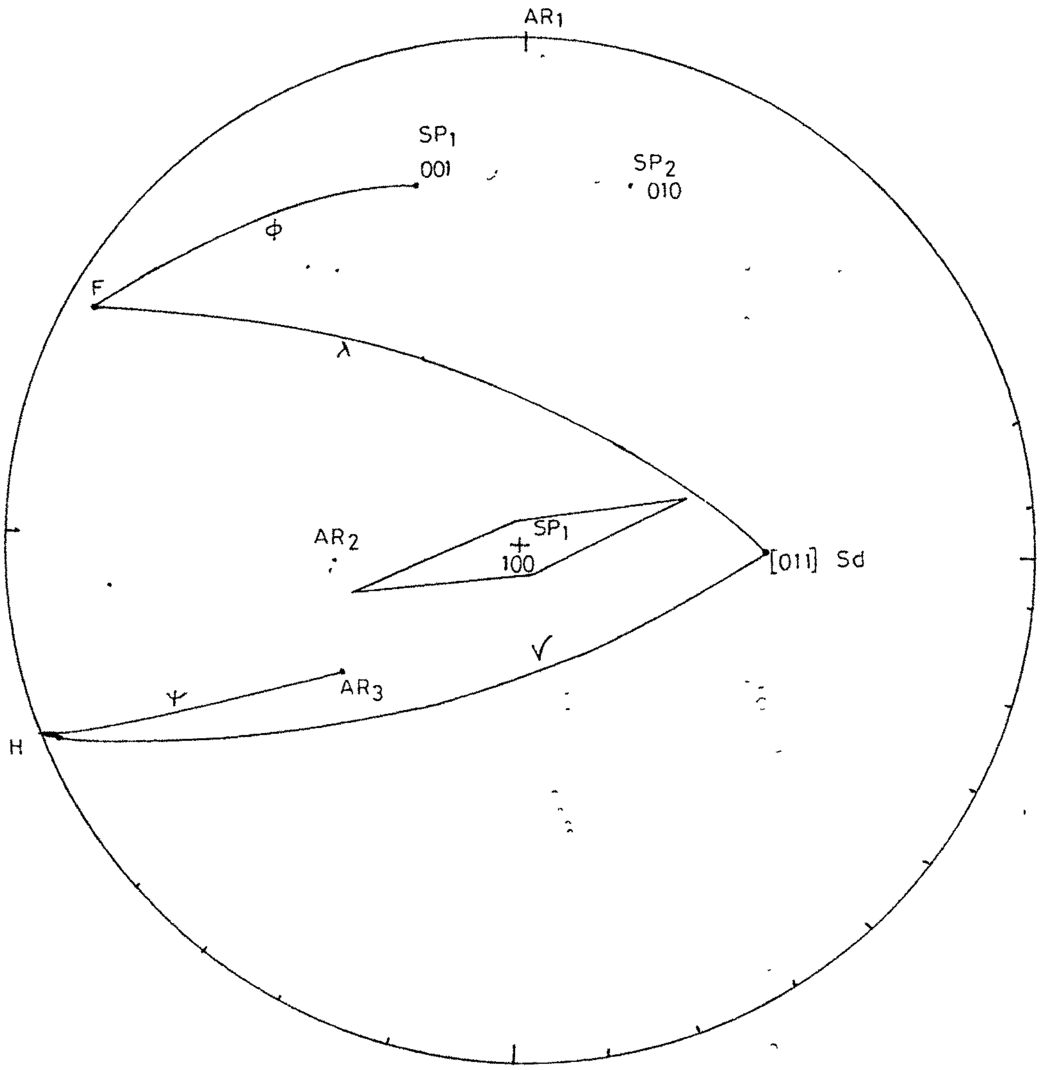

SLIP SYSTEM {100} [011]

Fig.: 7·1 (b)

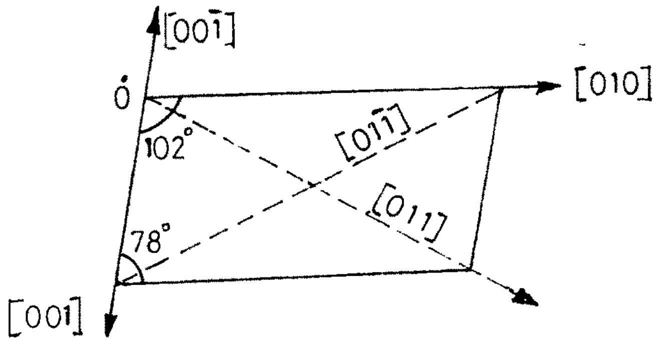

CONSIDERATION OF DIRECTION ACCORDING TO GALLAGHER et. al.

Fig.: 7·2 (a)

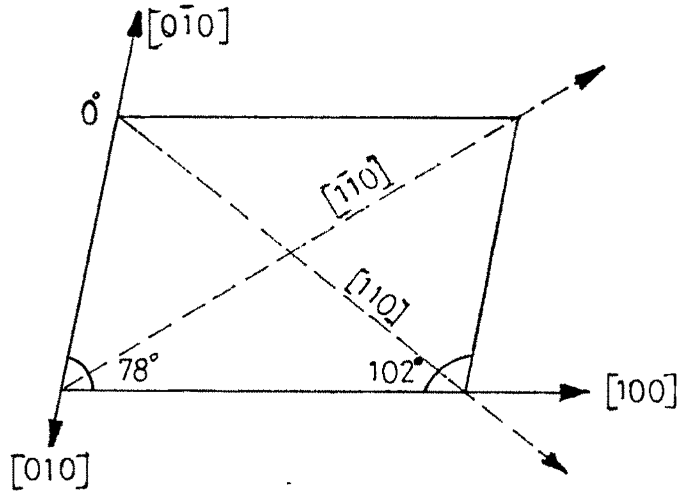

CONSIDERATION OF DIRECTION ACCORDING TO PRESENT WORK.

Fig.: 7·2 (c)

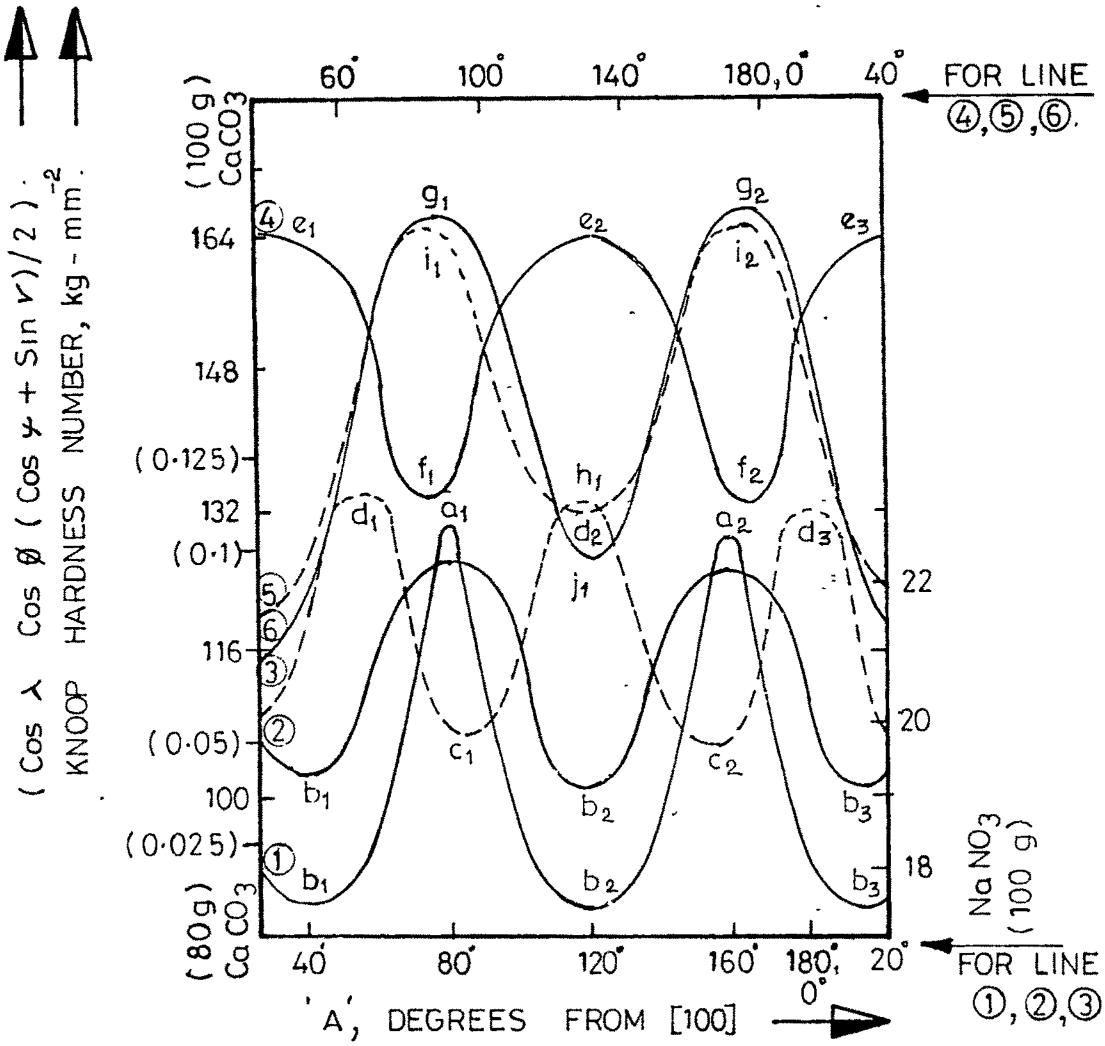

LINE – ① 'H' vs 'A' FOR $NaNO_3$ (BY PRESENT AUTHOR)
② 'H' vs 'A' FOR $CaCO_3$ (BY PRESENT AUTHOR)
③ 'ERSS' vs 'A' FOR $CaCO_3$ & $NaNO_3$ (BY PRESENT AUTHOR)
④ 'H' vs 'A' FOR $CaCO_3$ (BY GALLAGHER et al)
⑤ 'ERSS' vs 'A' FOR $CaCO_3$ & $NaNO_3$ (BY GALLAGHER et al.)
⑥ 'H' vs 'A' FOR $NaNO_3$ (BY GALLAGHER et al.)

ERSS VALUES CALCULATED USING 'B' OR EQUATION ASSUMING ACTIVE {100} [011] SLIP SYSTEM.

Fig.: 7·2 (b)

REFERENCES

1. C.A. Brookes; J.B. O'Neill and B.A.W. Redfern, Proc. R. Soc. London, Ser. A 322, 73 (1971)

2. F.W. Daniels and C.G. Dunn, Trans. Am. Soc. Metals, 41, 419 (1949)

3. C. Feng and C. Elbaum, Trans. AIME 212, 47, (1958)

4. M. Garfinkle and R.g. Garlick, Trans. AIME, 242, 809 (1968)

5. G.A. Sawyer; P.M. Sargent and T.F. Page, J. Mater. Sci., 15, 1001 (1978)

6. R.H.J. Hanninck; D.L. Kohlstedt and M.J. Murray, Proc. R. Soc. London, Ser. A 326, 409 (1972)

7. D.J. Rowcliffe and G.E. Hollox, J. Mater. Sci., 6, 1270 (1971)

8. S.G. Roberts; P.D. Warren and P.B. Hirsch, J. Mater. Res. 1(1), 162 (1986)

9. M. Schwartz; S.K. Nash and R. Zeman, Trans. TMS - AIME, 221, 554 (1961)

10. R.W.G. Wyckoff, Crystal Structure, Vol 2, 359, (Interscience, N.Y.) (1964)

11. J.M. Thomas and G.D. Renshaw, Trans. Faraday Soc., 61, 791 (1965)

12. R.E. Keith and J.J. Gilman, Acta. Metallurgica, 8, 1 (1960)

13. P. Braillon and J. Serughetti, Phys. Stat. Sol. (a) 36, 637 (1976)

14. H.g. Gallagher; A. Littlejohn; D.B. Sheen and J.N. Sherwood, Cryst. Latt. Def. and Amorph. Mat., 16, 137 (1987).